Available online at www.sciencedirect.com
ScienceDirect
Journal of Catalysis 243 (2006) 131–148
JOURNAL OF CATALYSIS
www.elsevier.com/locate/jcat

Solvent effects in liquid-phase reactions II. Kinetic modeling for citral hydrogenation

Samrat Mukherjee [1], M. Albert Vannice *

Department of Chemical Engineering, Pennsylvania State University, University Park, PA 16802-4400, USA

Received 28 April 2006; revised 14 June 2006; accepted 22 June 2006

Available online 22 August 2006

Abstract

The initial liquid-phase reaction to hydrogenate any of the three unsaturated bonds in the citral molecule can be described by a Langmuir–Hinshelwood (LH) mechanism that assumes that molecular citral and H atoms are the two most abundant reaction intermediates. It was applicable with each of the eight solvents studied; however, a wide range of values was obtained for the two adsorption equilibrium constants contained in the optimized rate equation, K_{cit} and K_{H_2}. Regarding the rate of overall citral disappearance, four possible solvent effects—mass transfer limitations, liquid-phase H_2 solubility, liquid-phase nonideality, and competitive solvent adsorption—were evaluated in detail to see whether one of them could account for the 3-fold variation in turnover frequency and possibly decrease the variation in adsorption equilibrium constants. Using the Weisz–Prater criterion established the absence of mass transfer limitations, using H_2 concentration provided no benefit, and including thermodynamic activity coefficients for citral gave only minimal benefit. However, introducing solvent adsorption into the site balance equation revealed that a narrow range exists for a single apparent rate constant that is applicable for all of the solvents, makes the K_{H_2} values essentially invariant, and reduces the range of K_{cit} values to a factor of 7. Kinetic studies at three temperatures gave adsorption equilibrium constants that provided consistent, meaningful values for the enthalpy and entropy of adsorption for citral, H_2, and the solvent. Consequently, this is the best single explanation for the observed kinetic behavior. Finally, individual rates of formation were calculated for the unsaturated alcohol (geraniol and nerol) versus the partially saturated aldehyde (citronellal) and the proposed LH model, either including or excluding competitive solvent adsorption, was able to describe each rate simultaneously using the same optimized adsorption equilibrium constants. Including the solvent in the rate expression again showed that a single set of apparent rate constants can exist that simultaneously describe the three reactions. Thermodynamic consistency of the adsorption equilibrium constants for citral, H_2, and the solvent was obtained in all cases.

1. Introduction

Selective hydrogenation of unsaturated compounds is an important category of organic reactions that impacts different sectors of the chemical industry. Most of the hydrogenation reactions in the pharmaceutical and fine chemical sectors are conducted in the liquid phase, where the solvent used can serve different functions such as dissolving reactants and products, controlling the reaction rate and any exothermicity, and imparting specific solvent–solute interactions that favor a higher rate and/or selectivity. For a heterogeneously catalyzed system, the solvent can also help maintain a clean catalyst surface by removing poisons or inhibitors.

The solvent can play an important role in a catalytic system, and most of the studies on solvent effects in hydrogenation reactions have been limited to interpretations based on solvent polarity or its acid–base properties [1–6], although a limited number of studies have dealt quantitatively with the kinetic aspects of solvent effects with a heterogeneous catalyst [7–10]. The present study examines solvent effects in the hydrogenation of citral, a model α,β-unsaturated aldehyde containing conjugated C=O and C=C bonds and an isolated C=C bond. Hydrogenation of unsaturated aldehydes can be a useful route for manufacturing unsaturated alcohols, which are commercially important compounds in the perfumery and specialty chemicals areas. Most studies on liquid-phase hydrogenation

* Corresponding author.
E-mail addresses: samrat.mukherjee@abbott.com (S. Mukherjee), mavche@engr.psu.edu (M.A. Vannice).
[1] Present address: Abbott Laboratories, N. Chicago, IL, USA.

0021-9517/$ – see front matter
doi:10.1016/j.jcat.2006.06.018

of these unsaturated aldehydes have focused on the activity and selectivity aspects arising from the type of catalyst used, rather than solvent effects [11–16]. In the current study, solvent effects were determined for citral hydrogenation in eight liquids: *n*-amyl acetate, ethyl acetate, *n*-hexane, cyclohexane, tetrahydrofuran, *p*-dioxane, ethanol, and cyclohexanol. These solvents were chosen based on their inactivity for hydrogenation under our reaction conditions and their significantly different physical and electronic properties. In part I of this study, kinetic data were obtained for citral hydrogenation on Pt/SiO_2 in these solvents in a regime free from mass transfer limitations, and the rate and selectivity characteristics were also presented [17]. The observed variation in the initial turnover frequency (TOF) among different solvents did not correlate with either the dielectric constant or the permanent dipole moment of the solvent [17]. This part of the investigation discusses modeling of the kinetic data obtained in the different solvents and examines the inclusion of solvent effects into the kinetic model.

2. Experimental

SiO_2 (Davison Grade 57) was used as the catalyst support after calcination in air at 773 K for 2 h. The 3.15% Pt/SiO_2 catalyst was prepared by ion exchange using tetraammine platinum(II) hydroxide hydrate, $Pt(NH_3)_4(OH)_2{\cdot}xH_2O$ (Aldrich Chem.), as the Pt-precursor, and then dried overnight in air in 393 K [17]. The dispersion of Pt was unity [17]. The catalyst was reduced at 673 K under flowing H_2 for 75 min before H_2 or CO chemisorption, and the same procedure was applied to pretreat the catalyst during the hydrogenation experiments.

The hydrogenation experiments were carried out in a 100-mL stainless steel semibatch autoclave reactor, and the catalyst pretreatment was done in situ to avoid any catalyst contamination before the reaction. The solvent and citral were purged with N_2 for 30 min to remove dissolved oxygen before being introduced into the reactor via a closed loop using a high-pressure syringe pump. Liquid samples were withdrawn from the reactor periodically and analyzed by gas chromatography as described previously [17]. The reactions were conducted in eight different solvents over a range of 298–423 K, 10–30 atm H_2, and 0.5–5.9 M citral, with reaction conditions of 373 K, 20 atm H_2 pressure, and 1 M citral concentration chosen to be the standard conditions at which the important reaction characteristics in these solvents were compared.

3. Results and discussion

The initial TOF for overall citral hydrogenation was evaluated based on the time derivatives of the citral concentration for conversions <20%. Under standard reaction conditions, initial TOF values exhibited a 2.5-fold variation among the different solvents, whereas this variation was a factor of 3.0 and 3.5 at 298 and 423 K, respectively, at the same reactant concentrations [17]. Fig. 1 shows rate dependencies on the H_2 pressure and the citral concentration at 373 K among the eight solvents. To model the kinetics of the reaction, initial TOF values were determined from runs at varying citral concentrations and hydrogen pressures in these different solvents.

3.1. Kinetic modeling

The reaction kinetics of citral hydrogenation on a Pt/SiO_2 catalyst have been modeled using a standard Langmuir–Hinshelwood (LH) mechanism [18]. Although LH kinetic models can have limitations due to the assumptions that are often made, they can be quite accurate over a specified range of reaction conditions and have been very successful in describing numerous heterogeneous catalytic systems [19,20]. Dihydrogen adsorption is dissociative on Pt, as it is on other noble metals [20]. In the simplest model, a single type of active site (S) is assumed to be available to both citral (Cit) and a hydrogen atom (H), and adsorption steps for the reactants were considered quasi-equilibrated [Eqs. (1) and (2)]. The reaction of the second adsorbed H atom with an adsorbed citral molecule [Eq. (4)] was assumed to be the rate-determining step (RDS), because it allows a rate expression with a maximum dependence of 1 on the H_2 activity [18]. The mechanism for the initial reaction to hydrogenate one of the unsaturated bonds can be expressed by the following elementary steps, written in terms of citral disappearance ($r = \sum r_j$):

$$H_2 + 2S \overset{K_{H_2}}{\rightleftharpoons} 2H\text{–}S, \tag{1}$$

$$Cit + S \overset{K_{cit}}{\rightleftharpoons} Cit\text{–}S, \tag{2}$$

$$Cit\text{–}S + H\text{–}S \overset{K_j^*}{\rightleftharpoons} HCit_j\text{–}S + S, \tag{3}$$

$$HCit_j\text{–}S + H\text{–}S \overset{k_j}{\rightarrow} H_2Cit_j\text{–}S + S, \tag{4}$$

$$H_2Cit_j\text{–}S \overset{1/K_{H_2cit_j}}{\rightleftharpoons} H_2Cit_j + S. \tag{5}$$

Here K_i represents the adsorption equilibrium constant for the ith species, whereas K_j^* and k_j are associated with one of the three initial reactions; however, hydrogenation of the isolated C=C double bond is minimal, and thus k is the sum of k_1 and k_2 for the RDS, as shown in Fig. 2, which contains only the principal constituents of the reaction network. The product H_2Cit_j in Eq. (5) refers to either the unsaturated alcohol (UALC), comprising two stereoisomers (geraniol and nerol), or the partially saturated aldehyde (PSALD), citronellal. *E*- and *Z*-citral were considered together in this regard, and no distinction was made between the relative reactivity of these two stereoisomers. The rate expression for overall citral disappearance based on the RDS [Eq. (4)] becomes ($\theta_i <$ fractional coverage of i)

$$r = L\left(\sum k_j \theta_{HCit_j}\right)\theta_H = LkK^*K_{cit}K_{H_2}C_{cit}P_{H_2}\theta_S^2, \tag{6}$$

where L represents the total number of active sites per gram of catalyst and $kK^* = \sum k_j K_j^*$. Although deactivation due to adsorption of byproducts—most likely CO—can occur [18], its effect on the initial rates is ignored here. If adsorbed H atoms and adsorbed citral molecules are assumed to be the only signif-

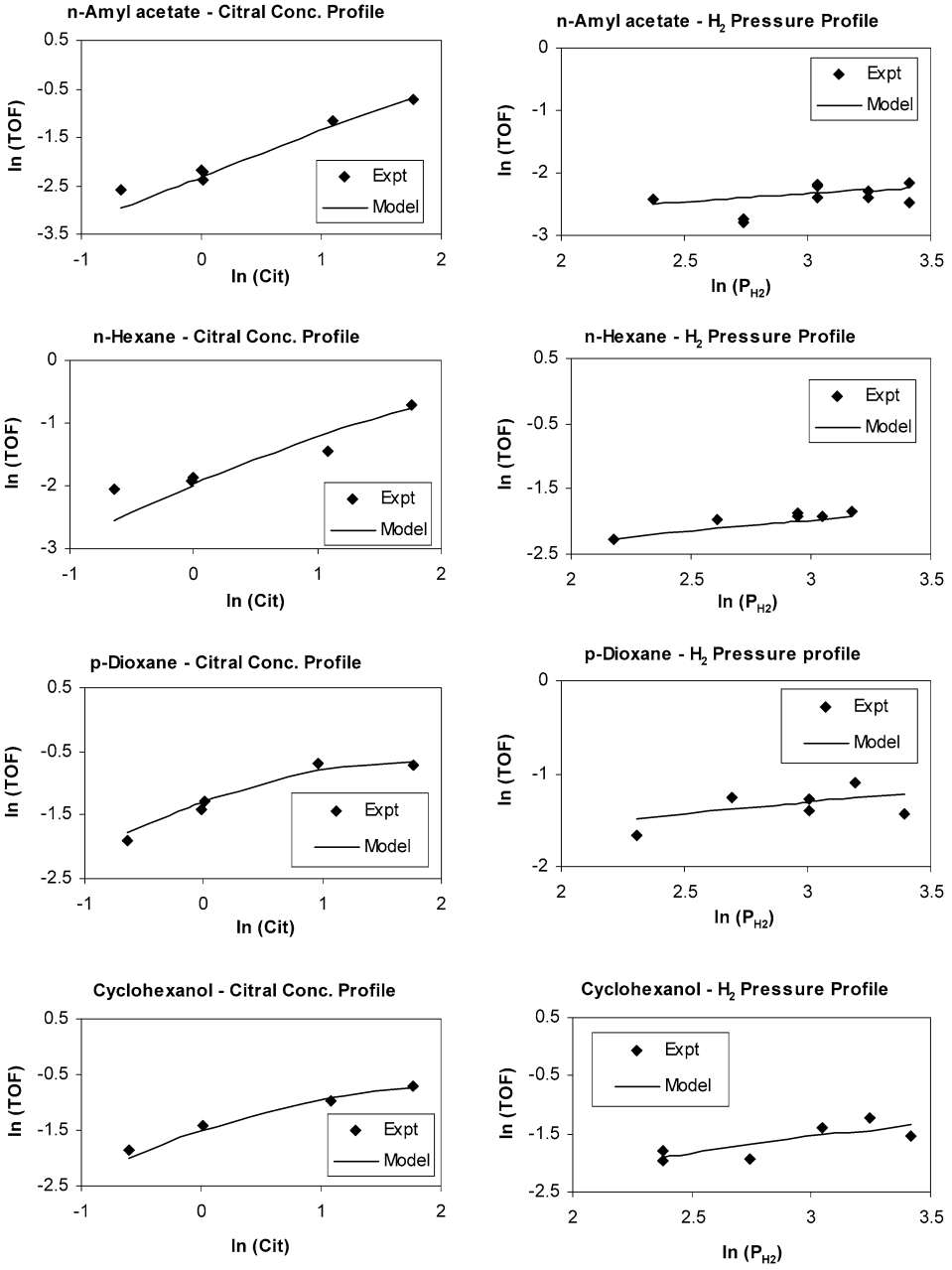

Fig. 1. Dependence of specific activity for citral consumption on citral concentration and H_2 pressure at 373 K in different solvents.

icant surface species in the site balance, then the TOF for citral disappearance can be written as [18,21]

$$\mathrm{TOF_{cit}} = \frac{r}{L} = \frac{kK^* K_{\mathrm{cit}} K_{\mathrm{H_2}} C_{\mathrm{cit}} P_{\mathrm{H_2}}}{[1 + K_{\mathrm{cit}} C_{\mathrm{cit}} + (K_{\mathrm{H_2}} P_{\mathrm{H_2}})^{0.5}]^2}. \quad (7)$$

This rate expression was used to model the initial rates of citral disappearance by using the initial citral concentration and the given hydrogen pressure at low citral conversion (<20%). The model-fitting parameters kK^*, K_{cit} and $K_{\mathrm{H_2}}$, were determined by a least squares fitting technique using a modified Powell algorithm; the optimization procedure was performed via a commercially available nonlinear regression package (MicroMath Scientist) [22]. Fig. 1 shows the fit of this model for the eight solvents at 373 K; Table 1 lists the optimized values of the three fitting parameters. The R^2 values of the regression coefficients are also listed to indicate goodness of fit. For this composite rate equation describing citral disappearance, K_{cit} and $K_{\mathrm{H_2}}$ varied by factors of 33 and 179, respectively, whereas the combined kK^* term showed a variation of 29. For two solvents, cyclohexane and ethyl acetate, similar runs were conducted at 298 and 423 K to allow evaluation of the thermodynamic properties of the adsorption equilibrium constants. These optimized values are provided in Table 2, Arrhenius plots of the adsorption constants are shown in Fig. 3, and the standard enthalpies and entropies of adsorption are listed in Table 3. All of the latter values satisfy all the rules and guidelines available for evaluating their consistency [20,23]. Consequently, although not proven, this reaction mechanism is reasonable and implies that

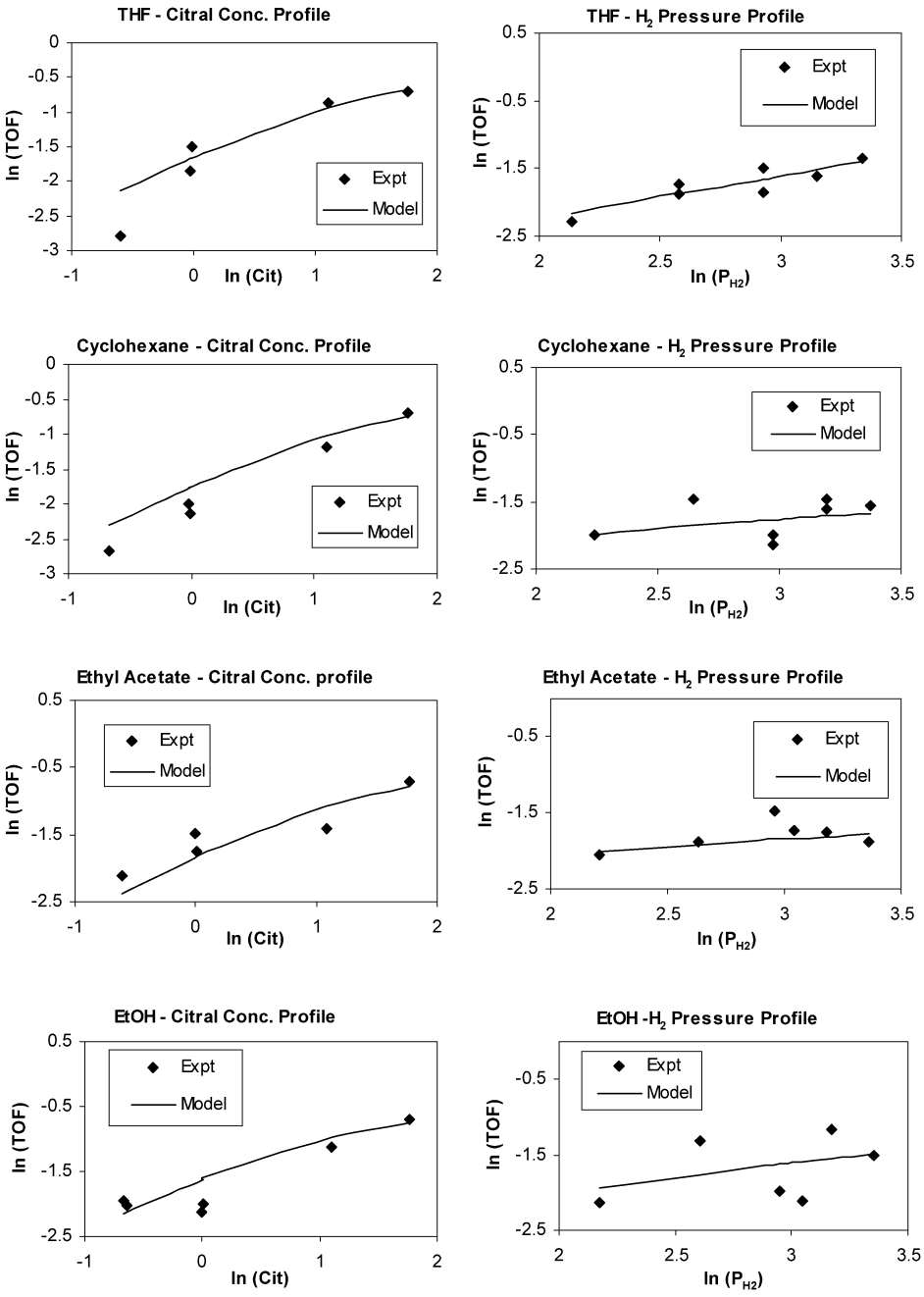

Fig. 1. (*continued*)

weakly bound hydrogen, with a heat of adsorption of around 6 ± 2 kcal mol^{-1}, is involved in the reaction. The heat of adsorption for citral is 16 ± 1 kcal mol^{-1}, which is near the value of 19 kcal/mol reported previously for another Pt/SiO_2 catalyst [18].

3.2. Solvent effects

3.2.1. Mass transfer limitations

The first solvent effect to consider is the possible influence of mass transfer due to differences in diffusivity in the liquid medium. We have verified that all data were obtained in the region of kinetic control [17].

3.2.2. Liquid-phase H_2 solubility

The next solvent effect to be considered is that related to H_2 solubility in the liquid medium. It has been shown that no external mass transport limitations exist at the high stirring speeds used here [17,22], so equilibrium between gas-phase and liquid-phase H_2 can be assumed, and Henry's law can be applied to calculate the mole fraction, x, of H_2 in the liquid phase, that is,

$$Hx_{H_2} = P_{H_2}. \tag{8}$$

Consequently, the H_2 adsorption process described by Eq. (1) can be separated into two steps,

$$H_{2(g)} \overset{1/H'}{\rightleftharpoons} H_{2(l)} \tag{1a}$$

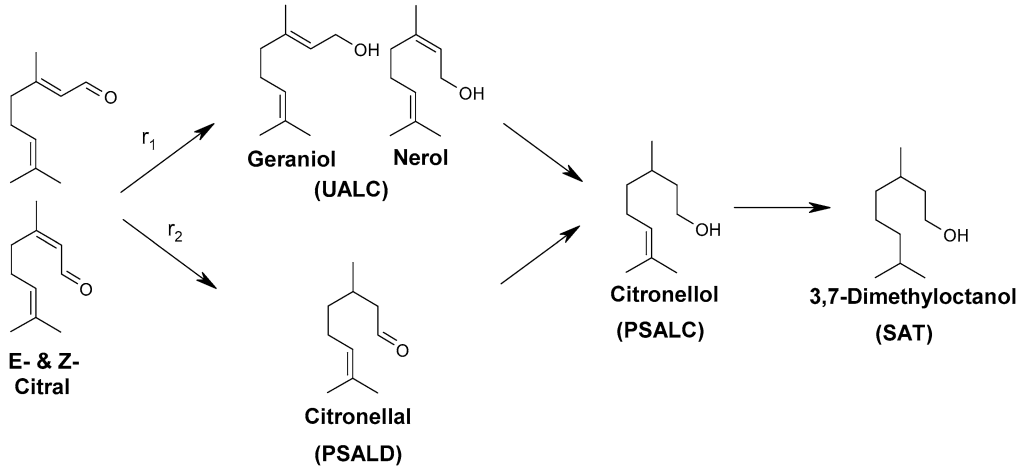

Fig. 2. The principal reaction chemistry for citral hydrogenation showing only the intermediates that were present in significant amounts.

Table 1
Optimal parameters in the LH rate expression [Eq. (7)] for overall citral hydrogenation at 373 K

Solvent	kK^* (s^{-1})	K_{cit} ($L\,mol^{-1}$)	K_{H_2} (atm^{-1})	R^2
Amyl acetate	2.9	0.063	0.41	0.98
Ethanol	0.92	0.53	0.37	0.99
Ethyl acetate	0.20	1.18	5.7	0.99
Cyclohexanol	2.9	0.33	0.071	0.99
Cyclohexane	0.56	0.59	0.90	0.99
n-Hexane	0.91	0.31	0.48	0.97
p-Dioxane	0.23	2.1	4.8	0.97
THF	5.6	0.23	0.032	0.95

Table 2
Optimized parameter values in the LH rate expression for overall citral hydrogenation in cyclohexane or ethyl acetate

Parameter	Solvent: Cyclohexane			Solvent: Ethyl acetate		
	298 K	373 K	423 K	298 K	373 K	423 K
K_{cit} ($L\,mol^{-1}$)	1.25	0.59	0.39	10.0	1.18	1.39
K_{H_2} (atm^{-1})	3.30	0.90	0.35	87.8	5.73	2.00
kK^* (s^{-1})	1.93	0.30	0.19	73.7	1.32	1.24

and

$$H_{2(l)} + 2S \overset{K'_{H_2}}{\rightleftharpoons} 2H\text{–}S, \tag{1b}$$

where H' is the Henry's law constant, H, converted to concentration units ($H' = HV_m$, where V_m is the molar volume at reaction conditions). Equation (7) then can be rewritten in terms of the H_2 concentration to correct for differences in H_2 concentration at the mouth of a catalyst pore, which gives

$$\mathrm{TOF} = r/L = \frac{kK^*K_{cit}K'_{H_2}C_{cit}C_{H_2}}{[1 + K_{cit}C_{cit} + (K'_{H_2}C_{H_2})^{0.5}]^2} = \frac{k'K_{cit}K'_{H_2}C_{cit}P_{H_2}}{[1 + K_{cit}C_{cit} + H'^{-0.5}(K'_{H_2}P_{H_2})^{0.5}]^2}, \tag{9}$$

where $k' = kK^*/H'$.

The solubility of H_2 in these pure solvents can be calculated by selected methods and can vary significantly, as indicated by the H' values listed in Table 4 as well as by previous studies [17,22]. For each run, the solubility of H_2 in the initial two-component mixture was calculated; based on regular solution theory [24], this is represented by the relationship

$$\ln H'_{mix} = x_1 \ln H'_1 + x_2 \ln H'_2 - a_{12}x_1x_2, \tag{10}$$

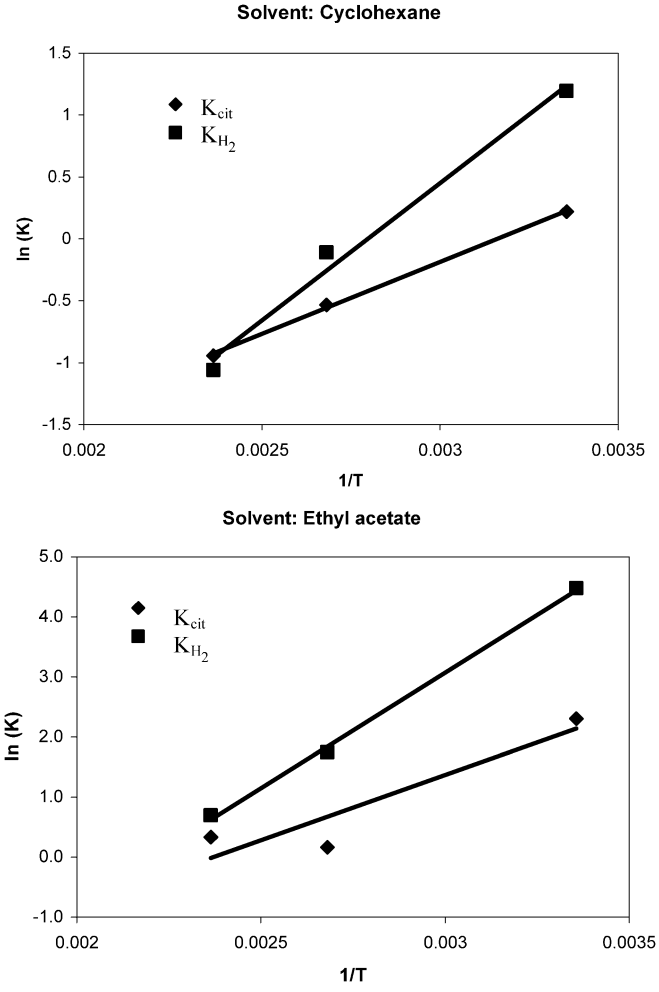

Fig. 3. Arrhenius plots of adsorption equilibrium constants from Table 2.

Table 3
Enthalpies and entropies of adsorption determined from rate parameters in Table 2 (standard state = 1 atm)

Solvent	Reactant	ΔH^0_{ad} (kcal mol^{-1})	ΔS^0_{ad} (cal mol^{-1} K^{-1})	S^0_{gas} (298 K) (cal mol^{-1} K^{-1})
Cyclohexane	Citral	−14.7	−28.5	130.0[a]
Cyclohexane	Hydrogen	−4.4	−12.3	31.2[b]
Ethyl acetate	Citral	−16.7	−31.2	130.0
Ethyl acetate	Hydrogen	−7.7	−16.8	31.2

[a] From Ref. [22].
[b] From Ref. [30].

where x_1 and x_2 are the respective mole fractions of citral and the solvent in the liquid phase, H'_1 and H'_2 are the respective Henry's law constants for H_2 dissolved in citral and the solvent, and a_{12} is a constant characteristic of the liquid pair, which can be estimated for nonpolar liquids as [24]

$$a_{12} = \frac{(\delta_1 - \delta_2)^2 (V_1^L + V_2^L)}{2RT}, \tag{11}$$

where δ_i is the solubility parameter [25] and V_i^L is the liquid molar volume of compound i. Including these Henry's law constants in Eq. (9) still leaves three adjustable fitting parameters, but it could narrow the range of values for the parameters in the rate expression if H_2 solubility were an important variable [8–10]. The fittings achieved using the H_2 concentration are shown in Fig. 4, and the optimized parameters are listed in Table 4. The R^2 values indicate little or no improvement, with the ranges of parameter values for k', kK^*, and K'_{H_2} even greater than those given in Table 1. This analysis demonstrates that H_2 solubility alone does not constitute an explanation for the range of rate parameters observed. Consequently, in our subsequent kinetic analyses, we will use H_2 pressure in the rate expressions.

3.2.3. Liquid-phase nonideality

A third possible solvent effect is the introduction of nonideal liquid-phase behavior due to solvent–solute interactions [19]. The citral concentration should then be replaced by its activity, a_{cit},

$$a_{cit} = \gamma_{cit} C_{cit}, \tag{12}$$

where γ_{cit} is the activity coefficient for a specific solvent. Various methods exist to calculate activity coefficients [26]; however, a UNIFAC-based method has been shown to be especially versatile in handling even highly nonideal solutions, such as those containing polar and associating molecules [27]. Consequently, activity coefficients for citral in the eight solvents at 373 K were estimated using a UNIFAC program based on interaction parameters of different functional groups in citral and the solvent; these values are listed in Table 5 along with the optimized parameter values when the activities for citral and H_2 are substituted into Eq. (7). Note that the activity coefficient for citral varies by a factor of 2.4 and, because dihydrogen behaves as an ideal gas under the reaction conditions, $a_{H_2} = P_{H_2}$. No significant improvement in fitting the data is achieved, because the regression coefficients are very similar. However, the range of kK^* and K_{cit} values is decreased somewhat, from 29 to 26 and from 33 to 31, respectively, whereas the range of K_{H_2} values is lowered significantly, from 179 to 27. Thus the use of thermodynamic activity rather than concentration does appear to be beneficial, as might be expected, but it still produces wide ranges of rate parameters.

3.2.4. Catalyst surface nonideality

Rather than assuming a Langmuirian surface with uniform sites, a nonuniform surface that can be altered by interactions with the solvent can be proposed to exist [19,22]. However, this approach is much more complicated and is discussed elsewhere [22], and thus it will not be pursued further here, primarily because the last solvent effect considered below can explain the observed behavior.

3.2.5. Competitive solvent adsorption

A fifth possible solvent effect is its competition for chemisorption on active sites even if the solvent is catalytically inert. Partial coverage of these sites would decrease overall activity, and differences in coverage among the solvents might account for the 3-fold variation in specific activity (TOF) that was observed. This effect can be readily incorporated into our LH model by assuming quasi-equilibrated adsorption of the solvents that is

$$\text{Solv} + \text{S} \overset{K_{solv}}{\rightleftharpoons} \text{Solv–S} \tag{1c}$$

Table 4
Optimized parameters in the LH rate expression for overall citral hydrogenation using H_2 concentrations [Eq. (9)]

Liquid	H'[a] (atm L mol^{-1})	k' (s^{-1} mol L^{-1} atm^{-1})	K_{cit} (L mol^{-1})	K'_H (L mol^{-1})	R^2
n-Amyl acetate	222	10.5	0.083	81.8	0.99
Ethanol	221	6.65	0.407	37.5	0.95
Ethyl acetate	165	0.571	2.33	2360	0.97
Cyclohexanol	306	12.2	0.281	16.8	0.98
Cyclohexane	216	2.24	0.673	224	0.97
n-Hexane	154	0.950	1.45	992	0.98
p-Dioxane	296	0.949	1.66	1140	0.99
THF	179	27.8	0.255	6.01	0.99
Citral	224				

Note. $T = 373$ K. Model equation: $\text{TOF} = \dfrac{k' K_{cit} K'_{H_2} C_{cit} P_{H_2}}{[1 + K_{cit} C_{cit} + H^{-0.5} (K'_{H_2} P_{H_2})^{0.5}]^2}$.

[a] Henry's law constant in pure solvent at 373 K (Ref. [22]).

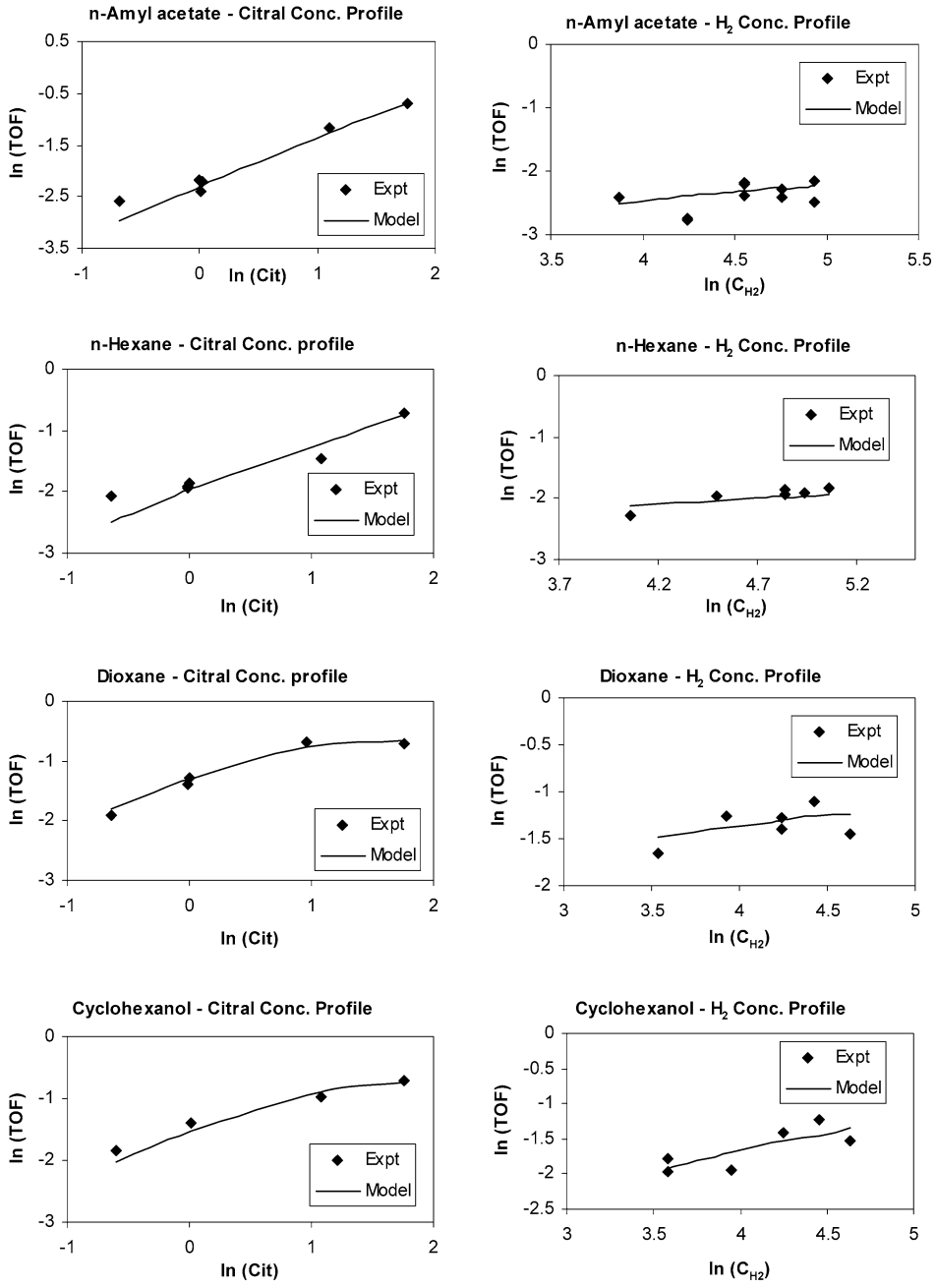

Fig. 4. Dependence of specific activity for citral consumption on the concentration of citral and H_2 at 373 K in different solvents.

and including a fractional coverage term for the solvent in the site balance, in addition to those for citral and hydrogen, to give

$$\theta + \theta_{\text{cit}} + \theta_{\text{H}} + \theta_{\text{solv}} = 1. \tag{13}$$

The final form of the LH rate expression with this term included is

$$\text{TOF}_{\text{cit}} = r/L = \frac{kK^{*}K_{\text{cit}}K_{\text{H}_2}C_{\text{cit}}P_{\text{H}_2}}{[1 + K_{\text{cit}}C_{\text{cit}} + K_{\text{solv}}C_{\text{solv}} + (K_{\text{H}_2}P_{\text{H}_2})^{0.5}]^2}. \tag{14}$$

Now, the total number of moles of organic compounds remains constant during any hydrogenation run, and if a negligible volume change occurs on mixing, then the initial solvent concentration from run to run can be expressed as a linear relationship of the citral concentration (mol L^{-1}),

$$C_{\text{solv}} = \alpha C_{\text{cit}} + \beta, \tag{15}$$

where $\alpha = -(\rho_{\text{solv}}M_{\text{cit}}/\rho_{\text{cit}}M_{\text{solv}})$ and $\beta = (\rho_{\text{solv}}/M_{\text{solv}})$, with ρ_i and M_i representing the liquid density (g L^{-1}) and the molecular weight (g mol^{-1}), respectively, for compound i. Table 6 lists these quantities for citral and the eight solvents used. Substituting this relationship into Eq. (7) and rearranging reveals that again there are only three independent fitting parameters,

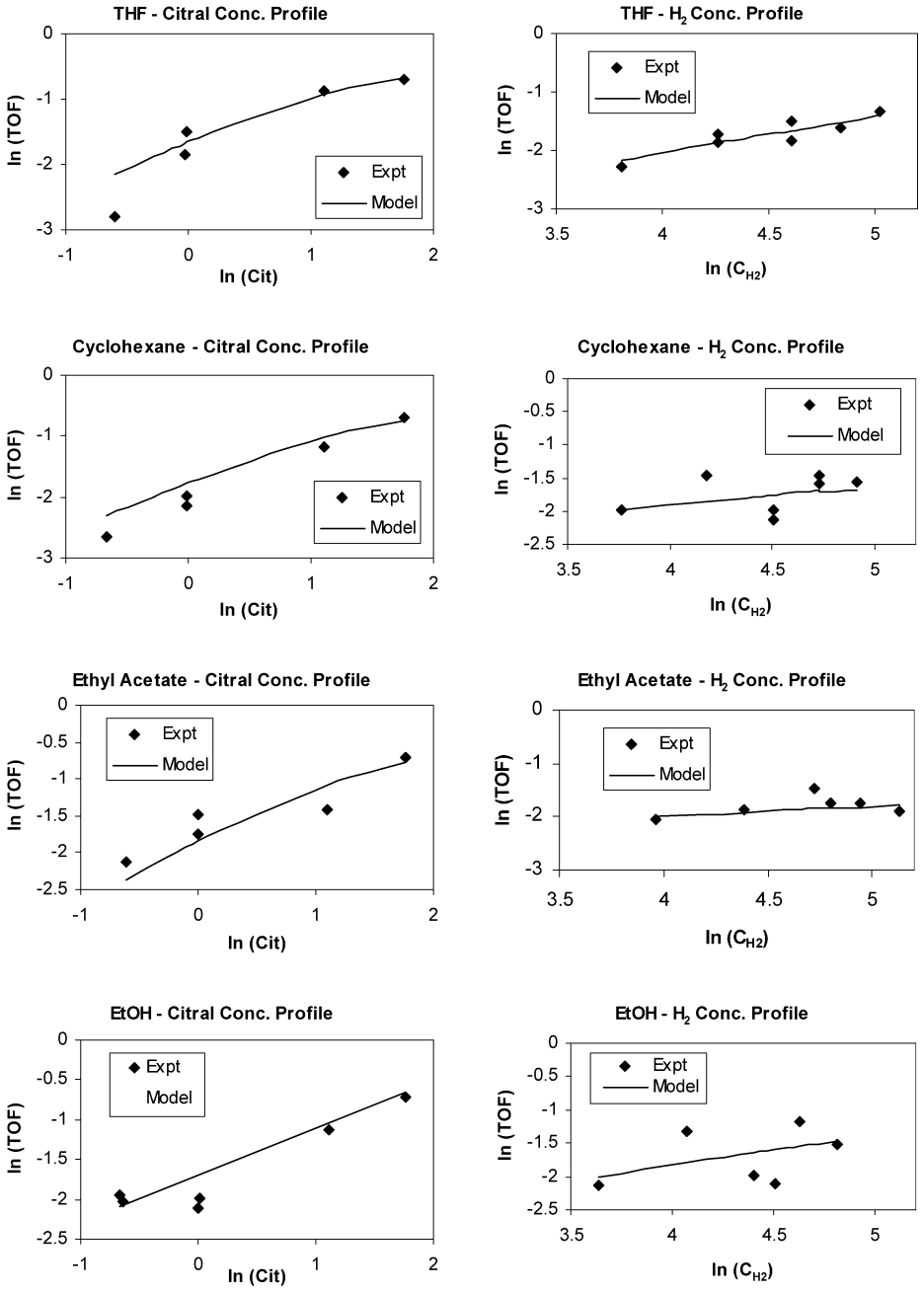

Fig. 4. (*continued*)

not four, as shown by the following rate equation:

$$\mathrm{TOF_{cit}} = \frac{r}{L} = \frac{\left(\frac{kK^*K_{\mathrm{cit}}K_{\mathrm{H_2}}}{(1+\beta K_{\mathrm{solv}})^2}\right)C_{\mathrm{cit}}P_{\mathrm{H_2}}}{\left[1+\left(\frac{K_{\mathrm{cit}}+\alpha K_{\mathrm{solv}}}{1+\beta K_{\mathrm{solv}}}\right)C_{\mathrm{cit}}+\left(\frac{K_{\mathrm{H_2}}^{1/2}}{1+\beta K_{\mathrm{solv}}}\right)P_{\mathrm{H_2}}^{1/2}\right]^2}. \quad (16)$$

The three optimized fitting parameters, p_i, are $p_1 = kK^* \times K_{\mathrm{cit}}K_{\mathrm{H_2}}/(1+\beta K_{\mathrm{solv}})^2$, $p_2 = (K_{\mathrm{cit}}+\alpha K_{\mathrm{solv}})/(1+\beta K_{\mathrm{solv}})$, and $p_3 = K_{\mathrm{H_2}}^{1/2}/(1+\beta K_{\mathrm{solv}})$, but they contain four unknown terms—kK^*, K_{cit}, $K_{\mathrm{H_2}}$, and K_{solv}—and the system is undetermined. However, if it is assumed that the energetics of the two H atom addition steps [Eqs. (3) and (4)] are not significantly affected by the different solvents, then kK^* is essentially constant, and the following question arises: "Is there a single value of kK^* that allows all of the rate expressions to be fit with meaningful values of K_{cit}, $K_{\mathrm{H_2}}$, and K_{solv}?" Using Mathematica, it can be shown that

$$K_{\mathrm{cit}} = \frac{\alpha p_1 - \beta p_1 p_2}{kK^*(\alpha-\beta p_2)\rho_3^2} = \frac{p_1}{kK^* p_3^2}, \quad (17)$$

$$K_{\mathrm{H_2}} = \left[\frac{\alpha kK^* p_3^2 - \beta p_1}{kK^*(\alpha-\beta p_2)p_3}\right]^2, \quad (18)$$

and

$$K_{\mathrm{solv}} = -\frac{p_1 + kK^* p_2 p_3^2}{kK^*(\alpha-\beta p_2)p_3^2}. \quad (19)$$

Obvious constraints can be placed on various values, that is, $p_i > 0$, $kK^* > 0$, $\alpha < 0$, $\beta > 0$, and K_{cit}, K_{H_2}, $K_{solv} > 0$. Because $K_{solv} > 0$, the numerator of Eq. (19) must be negative, so that $kK^* < p_1/p_2p_3^2$. This last inequality establishes that

$$0 < kK^* < p_1/p_2p_3^2. \tag{20}$$

The allowed values for kK^*, along with the three p_i values for each solvent, are listed in Table 6. The quality of the fits is the same as that given in Table 1. Only a narrow range between 0 and 0.195 provides values for kK^* that can simultaneously satisfy the rate expressions for all eight solvents. However, when similar inequalities are considered for each of the two initial parallel reactions, this range is decreased further, to 0.123 s^{-1} for consistency, as discussed in the following section. Regardless of the kK^* value chosen, the range of optimized K_{cit} values is essentially invariant at 7, whereas the range for K_{H_2} is markedly narrowed, to 1.8 ± 0.2. The only significant difference occurs in the range of K_{solv} values, which is decreased from 590 at $kK^* = 0.19$ to 16 at $kK^* = 0.001$. If an arbitrary, but reasonable, midrange value of $kK^* = 0.06$ s^{-1} is chosen as an example, then the corresponding K_{cit}, K_{H_2}, and K_{solv} values listed in Table 6 are obtained.

This analysis indicates that one possible explanation for the kinetic behavior obtained with these eight solvents is the influence of the solvent competing for adsorption on the surface sites. The constants in Table 6 imply that the weakest solvent adsorption (i.e., lowest K_{solv} values) occurs for ethyl acetate, *p*-dioxane, and ethanol, which provide three of the four highest rates at 373 K (17). The adsorption of H_2 does not seem to be altered much by the choice of solvent, as indicated by the relatively invariant K_{H_2} values of 63 $atm^{-1} \pm 24\%$ (mean value ± standard deviation). This approach markedly reduces the range of values for kK^*, K_{cit}, and K_{H_2} compared to those obtained with the first LH model (Table 1). The relatively invariant K_{H_2} values imply that these solvents have little effect on H_2 adsorption, and the range of K_{cit} values has been decreased from 33 (Table 1) to 7. As mentioned previously, kK^* must lie between 0 and 0.123 for the sum of $r_1 + r_2$ in Fig. 2 to be representative of the overall rate of citral consumption.

To further examine this model, Eq. (16) also can be applied to the rate data for citral disappearance in cyclohexane and ethyl acetate at 298, 373, and 423 K (Figs. 4 and 5 in part I of this study [17]). The optimized rate parameter values are given in Table 7; the $p_1/p_2p_3^2$ values show that at each temperature there is only a narrow range of kK^* values at any temperature that can apply to both solvents. If, as before, a midrange value in the overlapping region of kK^* is selected at each temperature, then the listed values of K_{cit}, K_{H_2}, and K_{solv} are obtained. These three midrange values of kK^* produce an Arrhenius plot indicating that $E - Q = 5.0$ kcal mol^{-1}; that is, the activation energy for the addition of the second H atom is 5.0 kcal mol^{-1} larger than the heat of reaction for the addition of the first H atom. Additional Arrhenius plots for the three adsorption equilibrium constants, shown in Fig. 5, provide the enthalpies and entropies of adsorption listed in Table 8. The heats of adsorption for citral and H_2 are essentially invariant at -18.3 ± 0.4 and -11.5 ± 0.1 kcal mol^{-1}, respectively, whereas this value for either solvent is noticeably lower than that for citral, as might be anticipated. The thermodynamic parameters in Table 8 again satisfy all of the rules available to evaluate them [20,23]. Although not proving this model, these results do exhibit kinetic and thermodynamic consistency and indicate that competitive adsorption of the solvent may be the best explanation for the varying rates observed with these eight solvents.

Table 5
Activity coefficients and optimized parameters in the LH rate expression for overall citral hydrogenation using activity rather than concentration in Eq. (7)

Solvent	X_{cit} [a]	γ_{cit} [b]	kK^* (s^{-1})	K_{cit} (L mol^{-1})	K_{H_2} (atm^{-1})	R^2
n-Amyl acetate	0.153	1.00	2.90	0.064	0.41	0.99
Ethanol	0.066	1.09	0.93	0.47	0.38	0.95
Ethyl acetate	0.106	0.94	0.18	1.34	6.39	0.96
Cyclohexanol	0.112	0.77	1.19	0.58	0.25	0.99
Cyclohexane	0.116	1.66	1.15	0.17	0.70	0.97
n-Hexane	0.137	1.64	4.66	0.043	0.24	0.99
p-Dioxane	0.094	1.86	0.36	0.71	2.73	0.98
THF	0.090	0.88	0.79	0.59	0.53	0.99

Note. $T = 373$ K, $a_{H_2} = P_{H_2}$.

Model equation: $\mathrm{TOF} = \dfrac{kK^* K_{cit} K_{H_2} a_{cit} P_{H_2}}{[1 + K_{cit} a_{cit} + (K_{H_2} P_{H_2})^{0.5}]^2}$.

[a] Mole fraction at 1 M citral.
[b] Estimated using UNIFAC.

3.3. Expansion of the initial citral hydrogenation model

One additional contribution from this simple LH model would be to describe the individual rates of formation of the

Table 6
Optimized parameters for Eq. (16) describing citral disappearance at 373 K

Solvent	p_1	p_2	p_3	α	β	$p_1/p_2p_3^2$	K_{cit} [a] (L mol^{-1})	K_{H_2} [a] (atm^{-1})	K_{solv} [a] (L mol^{-1})
n-Amyl acetate	0.0757	0.0633	0.641	−1.15	6.70	2.910	3.07	78.6	1.92
Ethanol	0.178	0.526	0.606	−2.93	17.1	0.924	8.10	51.7	0.635
Ethyl acetate	1.32	1.18	2.39	−1.73	10.1	0.195	3.84	50.4	0.194
Cyclohexanol	0.0676	0.332	0.267	−1.64	9.59	2.850	15.8	71.7	3.20
Cyclohexane	0.295	0.587	0.947	−1.57	9.19	0.560	5.48	49.8	0.702
n-Hexane	0.136	0.310	0.695	−1.30	7.62	0.910	4.70	49.6	1.20
p-Dioxane	2.27	2.08	2.20	−2.00	11.7	0.226	7.83	61.1	0.219
THF	0.0415	0.232	0.179	−2.09	12.2	5.590	21.6	93.5	4.35

[a] Evaluated at $kK^* = 0.06$ s^{-1}.

Table 7
Optimized parameters for Eq. (16) describing citral disappearance in cyclohexane and ethyl acetate

Solvent	T (K)	p_1	p_2	p_3	$p_1/p_2p_3^2$ [a]	kK^* (s^{-1})	K_{cit} [b] ($L\,mol^{-1}$)	K_{H_2} [b] (atm^{-1})	K_{solv} [b] ($L\,mol^{-1}$)
Ethyl acetate	298	73.7	10.0	9.37	0.084 (0.032)	0.016	52.5	2350	0.411
	373	1.32	1.18	2.39	0.195 (0.123)	0.06	3.84	50.4	0.194
	423	1.24	1.39	1.41	0.450 (0.44)	0.22	2.82	7.31	0.090
Cyclohexane	298	1.93	1.25	1.82	0.470 (0.032)	0.016	36.7	2228	2.72
	373	0.295	0.587	0.947	0.560 (0.123)	0.06	5.48	49.8	0.702
	423	0.185	0.390	0.589	1.37 (0.44)	0.22	2.42	7.43	0.395

[a] Values in parentheses are further constrained to be consistent with those for the individual initial rates.
[b] Evaluated at the cited kK^* value.

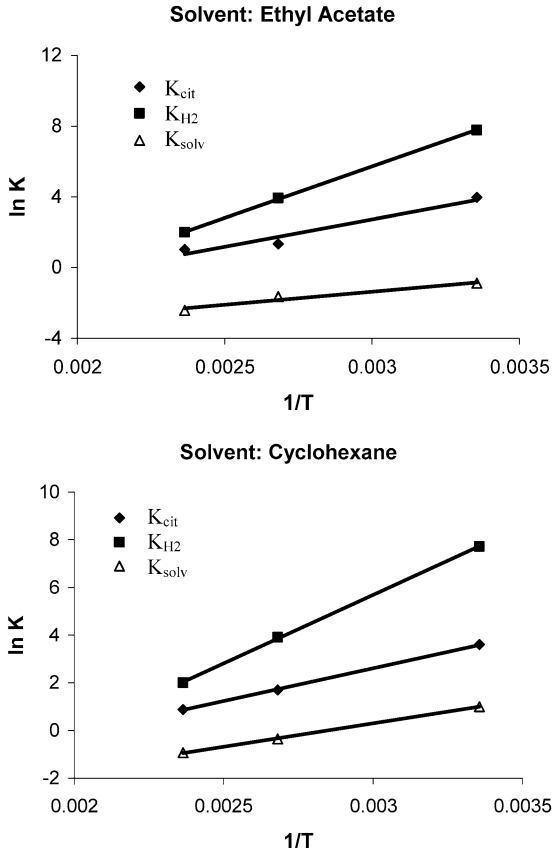

Fig. 5. Arrhenius plots of adsorption equilibrium constants for citral, H_2 and the solvent (from Table 7).

unsaturated alcohol (UALC), r_1, and the partially saturated aldehyde (PSALD), r_2, in addition to overall citral disappearance. As shown previously [17], initial hydrogenation of the isolated C=C bond to form 3,7-dimethyl-2-octenal (ENAL) is negligible and can be ignored. Using results such as those in Tables 2–4 in part I of this study [17], these two individual rates can be calculated if the relative rates of hydrogenation of UALC and PSALD can be determined. In an earlier study, hydrogenation of a 50% mixture of UALC and PSALD at 373 K showed that the competitive rate for citronellal hydrogenation was five times greater than that for geraniol [28]. Assuming that this ratio remains approximately constant over a range of reaction conditions, values of r_1 and r_2 can be estimated, and if the simplest approach is taken and solvent effects are ig-

Table 8
Enthalpies and entropies of adsorption determined from rate parameters in Table 7 (standard state = 1 atm)

Compound	ΔH^0_{ad} ($kcal\,mol^{-1}$)	ΔS^0_{ad} ($cal\,mol^{-1}\,K^{-1}$)	S^0_{gas} (298 K) ($cal\,mol^{-1}\,K^{-1}$)
Solvent: Cyclohexane			
Citral	−17.9	−32.2	130.0
H_2	−11.4	−22.9	31.2
Cyclohexane	−11.0	−30.8	71.1
Solvent: Ethyl acetate			
Citral	−18.6	−34.0	130.0
H_2	−11.5	−23.2	31.2
Ethyl acetate	−10.4	−32.5	86.0

Table 9
Optimized parameters in Eq. (7) for the LH model describing the individual formation of UALC (r_1) and PSALD (r_2) at 373 K

Solvent	$k_1K_1^*$ (s^{-1})	$k_2K_2^*$ (s^{-1})	K_{cit} ($L\,mol^{-1}$)	K_{H_2} (atm^{-1})	R^2
n-Amyl acetate	0.39	0.77	0.18	0.37	0.79
Ethanol	0.45	0.51	0.54	0.34	0.86
Ethyl acetate	0.033	0.091	2.3	6.2	0.77
Cyclohexanol	0.60	0.87	0.46	0.16	0.88
Cyclohexane	0.21	0.33	0.58	0.89	0.84
Hexane	0.20	0.46	0.55	0.40	0.77
Dioxane	0.13	0.44	1.4	0.57	0.83
THF	0.34	0.53	0.56	0.41	0.87

Table 10
Power law rate dependencies for UALC formation (r_1) and PSALD formation (r_2) at 373 K

Solvent	Rate: r_1		Rate: r_2	
	x_1	y_1	x_2	y_2
n-Amyl acetate	1.16	0.29	0.55	0.30
Ethanol	0.70	0.12	0.41	0.55
Ethyl acetate	0.75	0.04	0.25	0.30
Cyclohexanol	0.81	−0.12	0.17	0.88
Cyclohexane	1.15	0.36	0.48	0.26
Hexane	0.79	0.20	0.31	0.51
p-Dioxane	1.21	0.31	0.11	0.25
THF	1.09	0.75	0.55	0.62

Note. $r_j = C_{cit}^{x_j} P_{H_2}^{y_j}$.

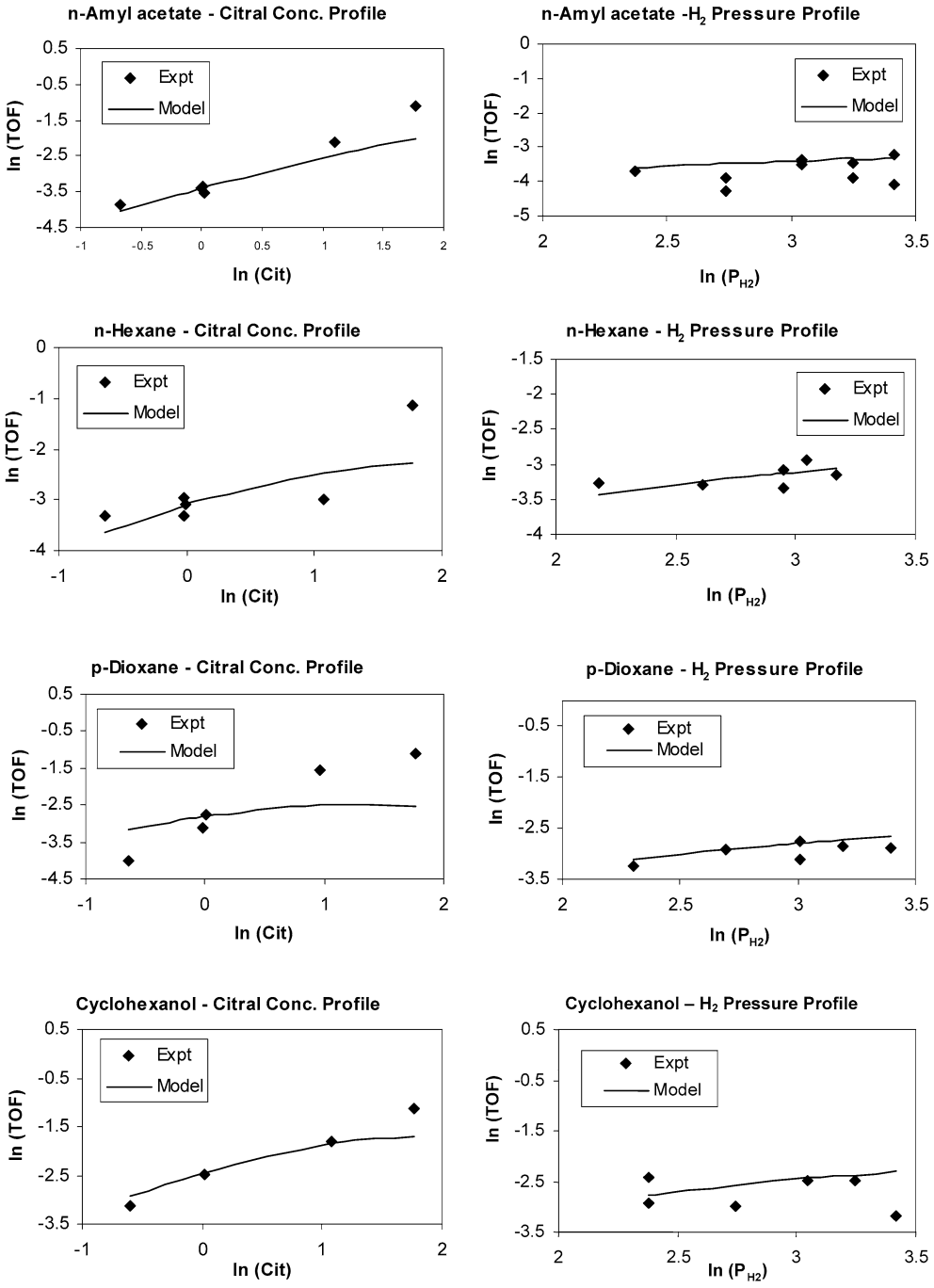

Fig. 6. Dependence of specific activity for unsaturated alcohol formation (r_1) on citral concentration and H_2 pressure at 373 K in different solvents.

nored, then Eq. (7) can be applied to each reaction individually. If only one type of active site is assumed, then the K_{cit} and K_{H_2} values must be the same for each reaction. With this constraint, simultaneous optimization of this equation to fit the two rates of formation gives the results shown in Figs. 6 and 7, and the optimized rate parameters are listed in Table 9 along with the R^2 values for the overall fits. Although the R^2 values are lower, the K_{cit} and K_{H_2} values are decreased, from 33 to 13 and from 179 to 38, respectively. Fitting the results in Figs. 6 and 7 to a power rate law yields the rate dependencies given in Table 10 for the two initial reactions. Note that the power law rate dependencies are sometimes significantly different for the two reactions, and they differ from the composite rate dependencies given previously for overall citral conversion [17]. Consequently, the values of the fitting parameters (i.e., the adsorption equilibrium constants) are not expected to be the same, although they often are similar. The fact that some of the y values are $>1/2$ eliminates a simple mechanism invoking addition of the first H atom as the RDS. Unfortunately, individual k_1 and k_2 values cannot be isolated. This same approach can be used to fit the data obtained with ethyl acetate and cyclohexane at 298 and 423 K. The relative hydrogenation rate for citronel-

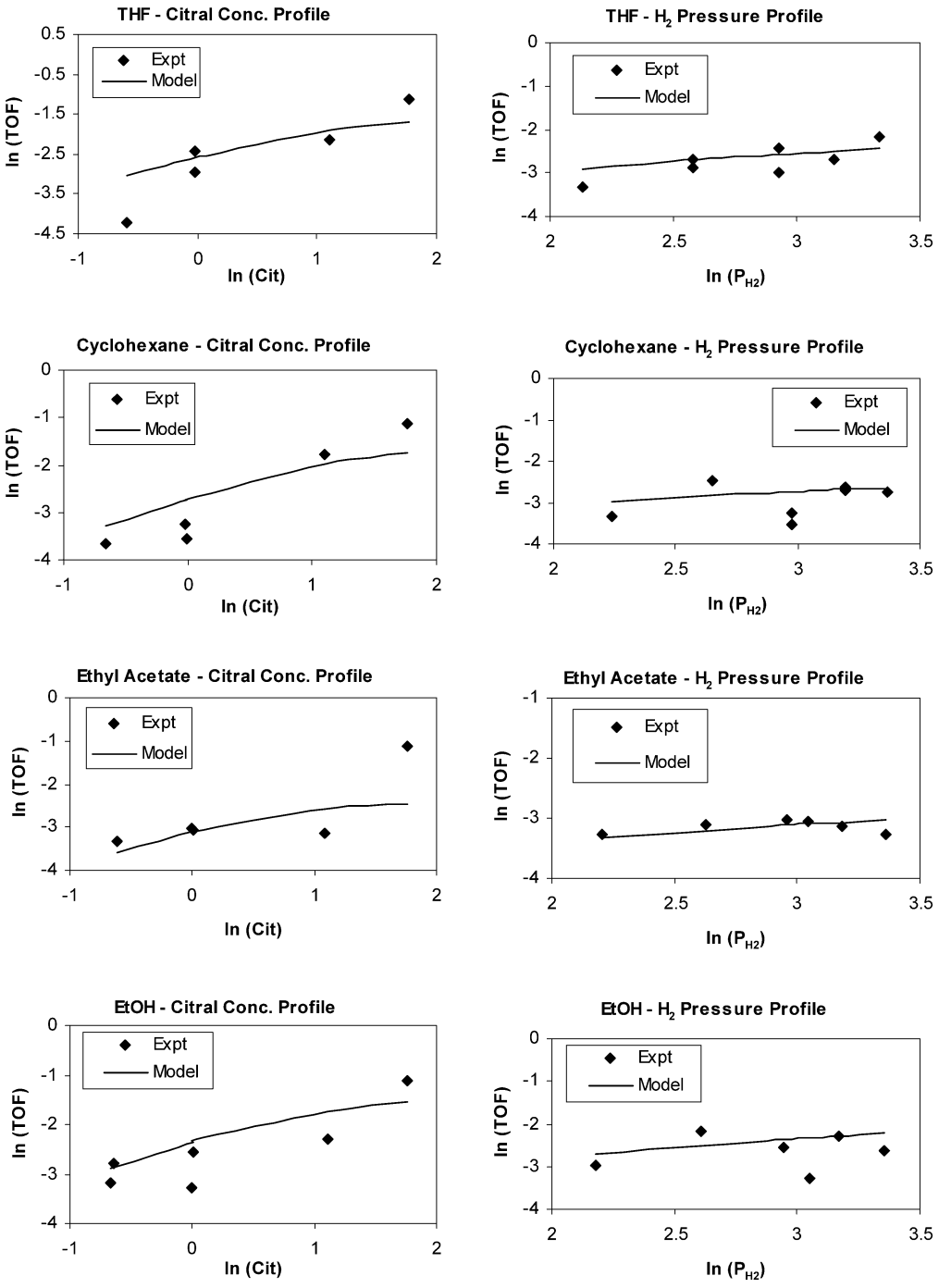

Fig. 6. (*continued*)

lal and geraniol was found to be $r_{\mathrm{PSALD}}/r_{\mathrm{UALC}} = r_2/r_1 = 0.44$ at 298 K [28], whereas the ratio of 5 measured at 373 K was used for 423 K. These results are shown in Figs. 8 and 9, and the fitting parameters are listed in Table 11. Arrhenius plots of the adsorption equilibrium constants provide the enthalpies and entropies of adsorption listed in Table 12. With this more detailed kinetic approach, the heat of adsorption of 18 kcal mol^{-1} for citral is again very close to that reported previously [18], whereas the Q_{ad} value of 11 kcal mol^{-1} for H_2 is near the value of 13.6 kcal mol^{-1} reported for the integral heat of adsorption of H_2 on Pt/SiO_2 catalysts [29].

Finally, one last improvement can be made to the kinetic model describing these two initial reactions by including solvent adsorption on active sites. Consequently, with this more complex model, equations identical to Eq. (16) can be written for the formation of unsaturated alcohol ($\mathrm{TOF_{UALC}} = r_{\mathrm{UALC}}/L = r_1/L$) and for the formation of partially saturated aldehyde ($\mathrm{TOF_{PSALD}} = r_{\mathrm{PSALD}}/L = r_2/L$), and a set of $p_{1,j}$, $p_{2,j}$, and $p_{3,j}$ values equivalent to that given in the preceding section can be obtained for each reaction, where $j = 1$ or 2. If the three adsorption equilibrium constants are same for each reaction, then $p_{2,1} = p_{2,2}$ and $p_{3,1} = p_{3,2}$, and the same in-

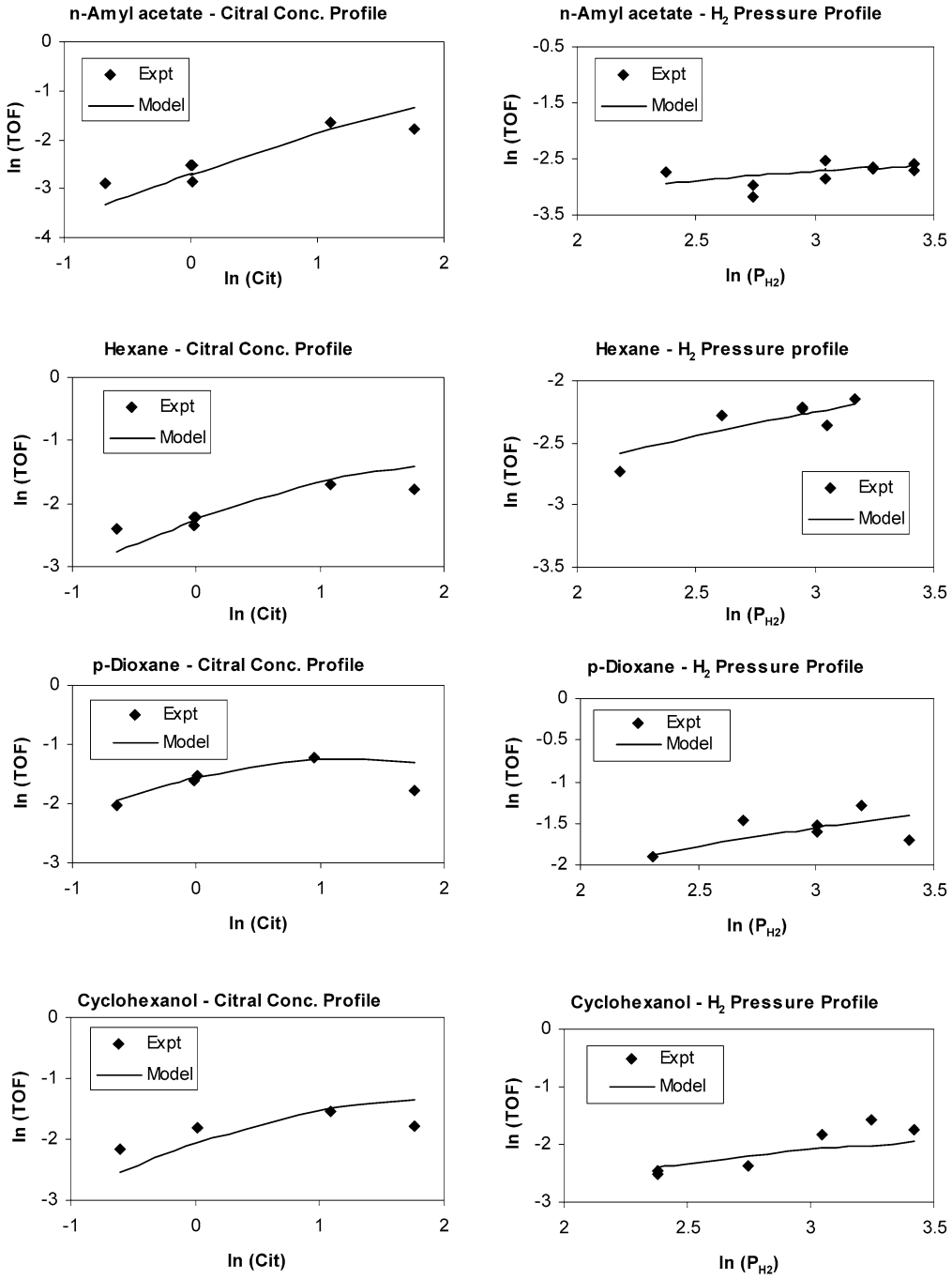

Fig. 7. Dependence of specific activity for citronellal formation (r_2) on citral concentration and H_2 pressure at 373 K in different solvents.

equality [Eq. (20)], still exists for each reaction, that is,

$$0 < k_1 K_1^* < p_{1,1}/p_2 p_3^2 \tag{21}$$

and

$$0 < k_2 K_2^* < p_{1,2}/p_2 p_3^2. \tag{22}$$

An examination of $p_{1,j}$ shows that

$$p_{1,1}/p_{1,2} = k_1 K_1^*/k_2 K_2^*, \tag{23}$$

and if the total rate is the sum of these two parallel initial rates, then $r = r_1 + r_2$ and

$$kK^* = k_1 K_1^* + k_2 K_2^*. \tag{24}$$

Combining Eqs. (23) and (24) shows that

$$k_1 K_1^* = kK^*/(1 + p_{1,2}/p_{1,1}) \tag{25}$$

and

$$k_2 K_2^* = kK^*/(1 + p_{1,1}/p_{1,2}). \tag{26}$$

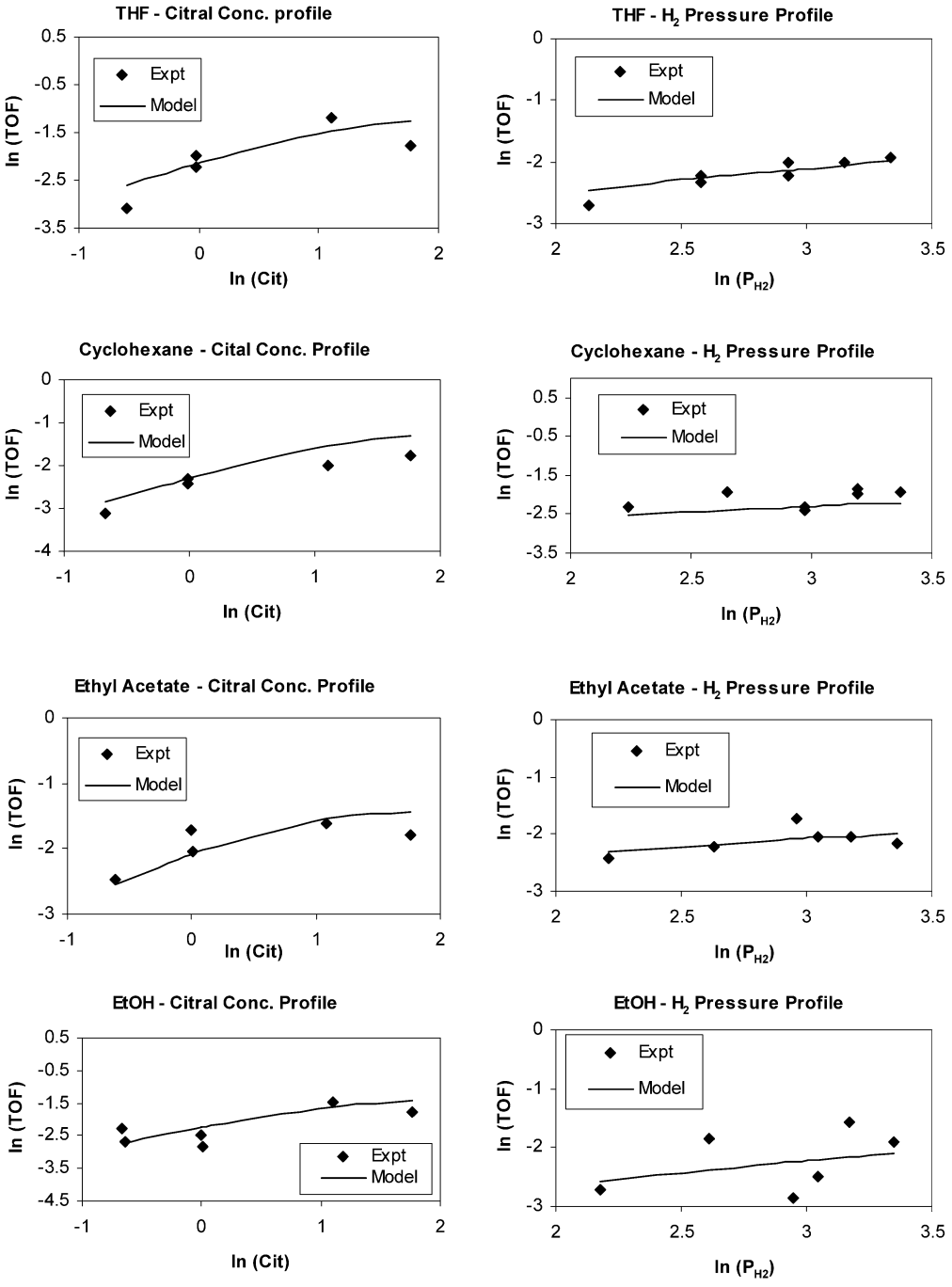

Fig. 7. (*continued*)

Therefore, once a value of kK^* is selected for the overall rate, values for $k_j K_j^*$ are determined automatically, and a single set of values is applicable for all three reaction sequences; however, all three values must satisfy the inequalities represented by Eqs. (20)–(22). The latter two are more constraining, and they decrease the maximum values of kK^* to 0.0316 s^{-1} at 298 K, 0.123 s^{-1} at 373 K, and 0.439 s^{-1} at 423 K. As a reasonable example, a midrange value for kK^* was selected at each temperature; these are the values used in Tables 6, 7, 13, and 14. Table 13 lists the optimized fitting parameters, gives the maximum allowable values for $k_j K_j^*$, and provides values for the three adsorption equilibrium constants at 373 K. Table 14 extends these calculations to 298 and 423 K. With these latter parameters at three temperatures, the Arrhenius plots shown in Fig. 10 give the enthalpy and entropy of adsorption values given in Table 15. Compared with the same values in Table 12, which were determined neglecting the solvent, ΔH_{ad}^0 values for citral and H_2 remain essentially unchanged, although that for H_2 is now more similar in the two solvents, and these values are almost identical to those in Table 8. The ΔH_{ad}^0 values in Table 15 for the two solvents are quite similar and much lower than that for citral, as would be anticipated, and they

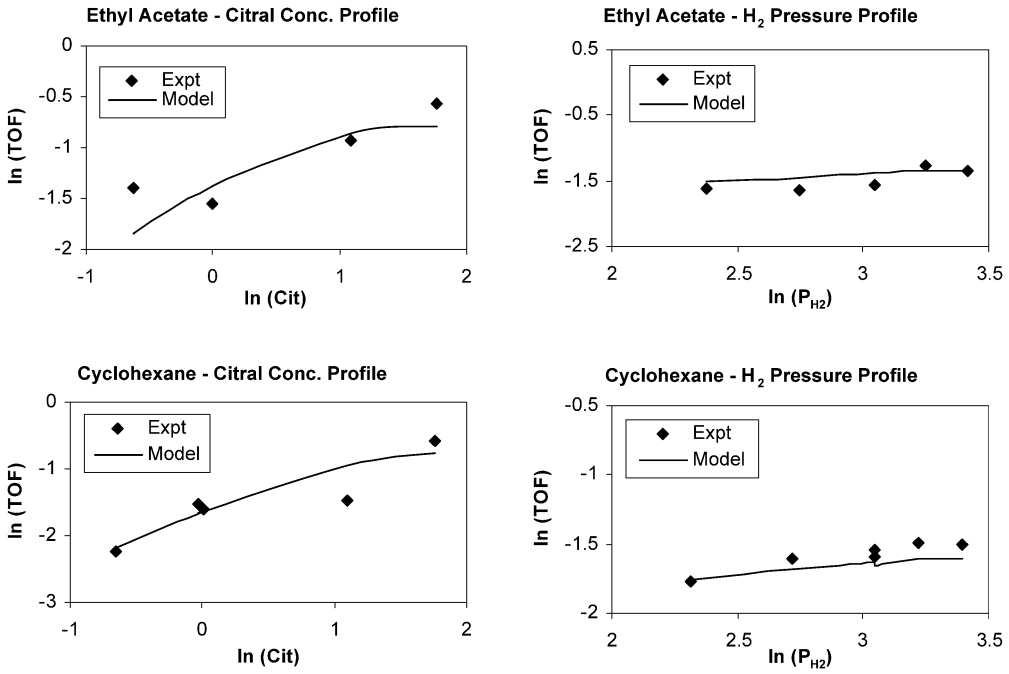

(a)

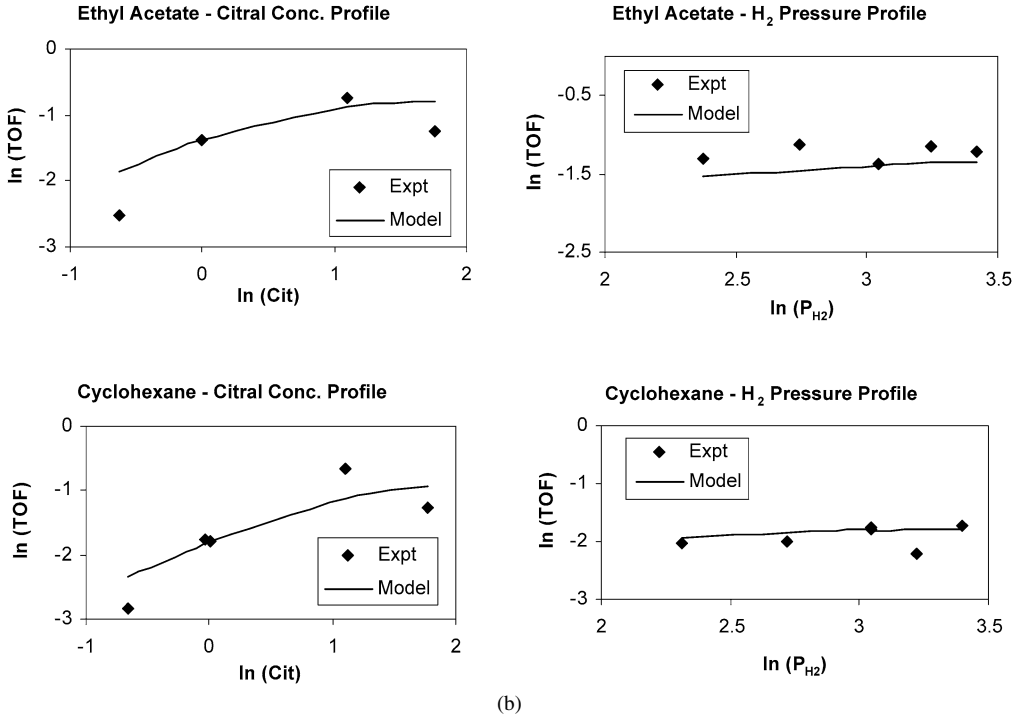

(b)

Fig. 8. (a) Fit of Eq. (7) to UALC formation (r_1) at 298 K in either ethyl acetate or cyclohexane. (b) Fit of Eq. (7) to PSALD formation (r_2) at 298 K in either ethyl acetate or cyclohexane.

are lower than those shown in Table 8. An Arrhenius analysis of the midrange choice of kK^* values yielded (E–Q) values of 4.1 ± 0.1 kcal mol^{-1} for $k_1 K_1^*$ and 5.7 ± 0.1 kcal mol^{-1} for $k_2 K_2^*$, indicating a somewhat lower net energy barrier for the formation of the unsaturated alcohols. As mentioned previously, these kinetic parameters and the thermodynamic values in Tables 12 and 15 are very insensitive to the choice of kK^* value.

4. Summary

The initial liquid-phase citral hydrogenation reaction to hydrogenate any one of the three unsaturated bonds in the molecule can be described by a straightforward LH mechanism that assumes that molecular citral and H atoms are the two most abundant reaction intermediates. This model was applicable with each of the eight different solvents studied, and an approxi-

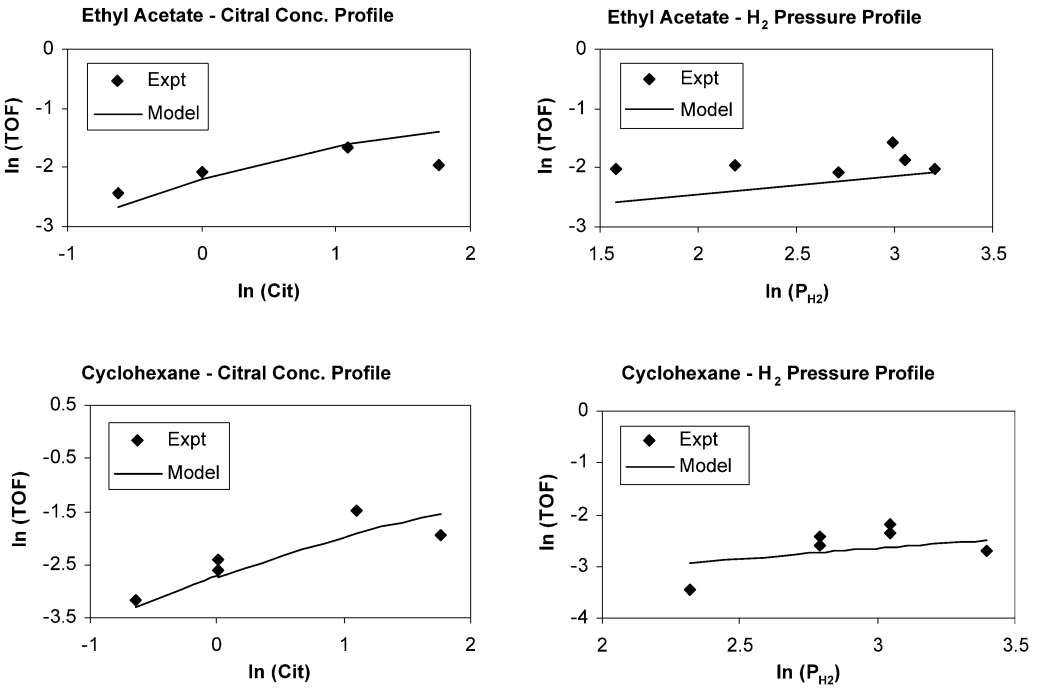

(a)

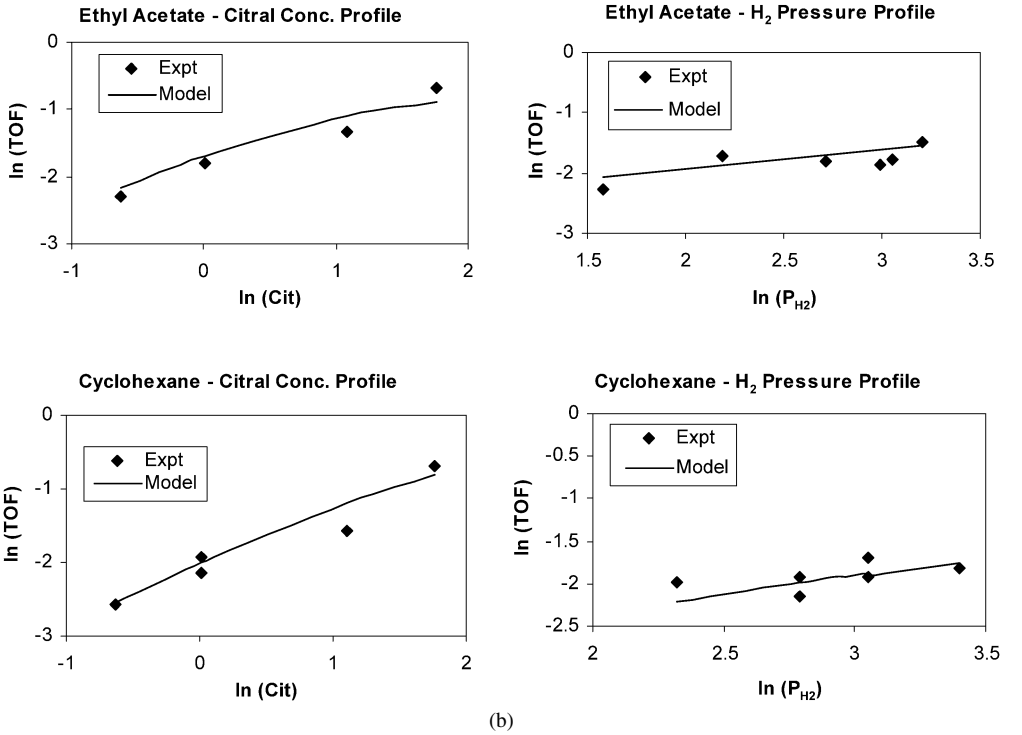

(b)

Fig. 9. (a) Fit of Eq. (7) to UALC formation (r_1) at 423 K in either ethyl acetate or cyclohexane. (b) Fit of Eq. (7) to PSALD formation (r_2) at 423 K in either ethyl acetate or cyclohexane.

mately 3-fold variation was found among the TOFs. In addition, a wide range of values was observed for each of the three fitting parameters in the different solvents, including the adsorption equilibrium constants for citral and H_2.

Five solvent effects were proposed, and four of these were evaluated in detail to see whether one of them could account for the variation in specific activity and possibly decrease the range of values obtained for the fitting parameters. Experiments and use of the Weisz–Prater (WP) criterion eliminated mass transfer effects as a possible explanation; use of the liquid-phase H_2 concentration, rather than H_2 pressure, in the rate expression provided no benefit. Assuming liquid-phase non-ideal behavior for the citral/solvent system and hence using thermodynamic activity rather than concentration in the rate expression provided minimal improvement in fitting capability, but did reduce the range of values for the fitting parameters,

Table 11
Optimized parameter values in the LH rate expression [Eq. (7)] for UALC (r_1) and PSALD (r_2) formation in ethyl acetate or cyclohexane at 298 and 423 K

Solvent	$k_1K_1^*$ (s^{-1})	$k_2K_2^*$ (s^{-1})	K_{cit} ($L\,mol^{-1}$)	K_{H_2} (atm^{-1})	R^2
Ethyl acetate (298 K)	0.0159	0.0157	23.1	628	0.95
Ethyl acetate (423 K)	0.164	0.275	1.32	2.23	0.94
Cyclohexane (298 K)	0.0750	0.0632	3.60	33.3	0.92
Cyclohexane (423 K)	0.698	1.45	0.272	0.197	0.95

Table 12
Enthalpies and entropies of adsorption determined from K_{cit} and K_{H_2} values in Tables 9 and 11 (standard state = 1 atm)

Reactant	ΔH_{ad}^0 ($kcal\,mol^{-1}$)	ΔS_{ad}^0 ($cal\,mol^{-1}\,K^{-1}$)
Solvent: Cyclohexane		
Citral	−17.6	−36.1
Hydrogen	−10.3	−27.8
Solvent: Ethyl acetate		
Citral	−18.3	−34.7
Hydrogen	−11.8	−27.2

especially K_{H_2}. The last explanation considered—competitive solvent adsorption—introduced an additional term into the LH rate expression via the site balance, and it was shown that at any temperature, a single kK^* value exists within a narrow range of such values that is applicable to all of the solvents and allows for the possibility that the energetics for addition of the

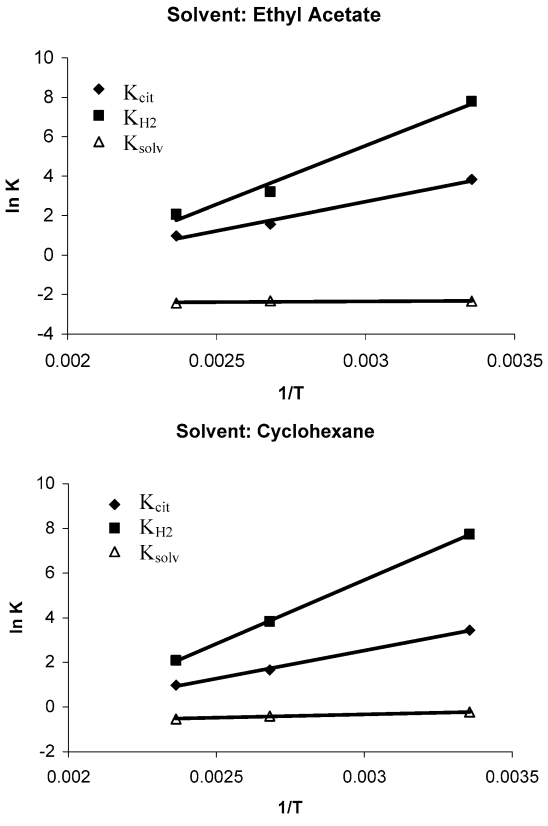

Fig. 10. Arrhenius plots of adsorption equilibrium constants for citral, H_2 and the solvent from Table 14.

Table 13
Optimized parameters in Eq. (16) for the LH model describing the individual formation of UALC (r_1) and PSALD (r_2) at 373 K

Solvent	$p_{1,1}$	$p_{1,2}$	p_2	p_3	$p_{1,1}/p_2p_3^2$	$p_{1,2}/p_2p_3^2$	$k_1K_1^{*a}$ (s^{-1})	$k_2K_2^{*a}$ (s^{-1})	K_{cit} ($L\,mol^{-1}$)	K_{H_2} (atm^{-1})	K_{solv} ($L\,mol^{-1}$)
n-Amyl acetate	0.0250	0.0498	0.175	0.607	0.387	0.770	0.0201	0.0399	3.38	38.8	1.38
Ethanol	0.0811	0.0921	0.539	0.581	0.445	0.506	0.0281	0.0319	8.55	50.9	0.659
Ethyl acetate	0.468	1.31	2.33	2.49	0.033	0.091	0.0158	0.0442	4.80	24.5	0.0977
Cyclohexanol	0.0450	0.0650	0.460	0.402	0.604	0.873	0.0245	0.0355	11.3	53.7	1.80
Cyclohexane	0.110	0.170	0.582	0.944	0.212	0.328	0.0236	0.0364	5.24	45.9	0.673
n-Hexane	0.0431	0.102	0.554	0.632	0.195	0.461	0.0178	0.0422	6.06	29.5	0.998
p-Dioxane	0.102	0.350	1.40	0.755	0.129	0.440	0.0136	0.0464	13.2	41.7	0.647
THF	0.0758	0.119	0.556	0.636	0.337	0.527	0.0234	0.0366	8.00	51.2	0.840

[a] Evaluated at $kK^* = 0.06\ s^{-1}$.

Table 14
Optimized parameters in Eq. (16) for the LH model describing the individual formation of UALC (r_1) and PSALD (r_2) in cyclohexane and ethyl acetate

T (K)	$p_{1,1}$	$p_{1.2}$	p_2	p_3	$p_{1,1}/p_2p_3^2$	$p_{1,2}/p_2p_3^2$	$k_1K_1^*$ (s^{-1})	$k_2K_2^*$ (s^{-1})	K_{cit} ($L\,mol^{-1}$)	K_{H_2} (atm^{-1})	K_{solv} ($L\,mol^{-1}$)
Solvent: Ethyl acetate											
298	230	228	23.1	25.1	0.016	0.016	0.00804[a]	0.00796	45.6	2437	0.0956
373	0.468	1.31	2.33	2.49	0.033	0.091	0.0158[b]	0.0442	4.80	24.5	0.0977
423	0.484	0.810	1.32	1.49	0.164	0.275	0.0823[c]	0.138	2.63	7.91	0.0869
Solvent: Cyclohexane											
298	9.00	7.58	3.60	5.77	0.075	0.063	0.00868[a]	0.00732	31.1	2291	0.794
373	0.110	0.170	0.582	0.944	0.212	0.328	0.0236[b]	0.0364	5.24	45.9	0.673
423	0.0374	0.0778	0.272	0.444	0.698	1.452	0.0714[c]	0.149	2.66	8.04	0.586

[a] Evaluated at $kK^* = 0.016\ s^{-1}$.
[b] Evaluated at $kK^* = 0.06\ s^{-1}$.
[c] Evaluated at $kK^* = 0.22\ s^{-1}$.

Table 15
Enthalpies and entropies of adsorption determined from rate parameters in Table 14 (standard state = 1 atm)

Compound	ΔH^0_{ad} (kcal mol^{-1})	ΔS^0_{ad} (cal mol^{-1} K^{-1})	S^0_{gas} (298 K) (cal mol^{-1} K^{-1})
Solvent: Cyclohexane			
Citral	−17.4	−30.9	130.0
H_2	−11.4	−22.8	31.2
Cyclohexane	−7.7	−22.2	71.1
Solvent: Ethyl acetate			
Citral	−18.3	−33.2	130.0
H_2	−11.8	−24.4	31.2
Ethyl acetate	−7.6	−26.2	86.0

first H_2 molecule to citral are the same in all solvents and the 3-fold variation in rate is due only to solvent coverage of active sites. This kinetic approach reduces the range of K_{cit} to only a 7-fold variation and makes the K_{H_2} value essentially invariant, implying that the solvent has little influence on H_2 adsorption. Adsorption equilibrium constants obtained at different temperatures provided consistent, meaningful values for the enthalpy and entropy of adsorption for citral, H_2, and the solvent. Consequently, solvent competition for adsorption sites appears to be the best singular explanation for the kinetic behavior observed.

Finally, by incorporating previously reported rate data, individual rates of formation for geraniol and nerol (UALC) versus citronellal (PSALD) were calculated, and the LH model proposed (either excluding or including solvent adsorption) was shown to be able to describe each rate simultaneously using the same optimized adsorption equilibrium constants in each rate expression. Inclusion of the solvent again left one undetermined parameter—an apparent rate constant—but these two equations narrowed the range of universally acceptable rate constant (kK^*) values and again allowed the possibility of a single rate constant being applicable for each reaction. The selection of reasonable, midrange values at each temperature produced thermodynamically consistent adsorption equilibrium constants with heats and entropies of adsorption very consistent with literature values.

References

[1] M.A. Aramendia, V. Borau, C. Jimenez, J.M. Marinas, A. Porras, F. Urbano, J. Catal. 172 (1997) 46.
[2] R.A. Rajadhyaksha, S.L. Karwa, Chem. Eng. Sci. 41 (1986) 1765.
[3] M.J. Vaidya, S.M. Kulkarni, R.V. Chaudhari, Org. Proc. Res. Dev. 7 (2003) 202.
[4] J.P. Wauquier, J.C. Jungers, Bull. Soc. Chim. Fr. 1280 (1957).
[5] H. Yamada, S. Goto, J. Chem. Eng. Jpn. 36 (2003) 586.
[6] H. Takagi, T. Isoda, K. Kusakabe, S. Morooka, Energy Fuels 13 (1999) 1191.
[7] S. Kishida, S. Teranishi, J. Catal. 12 (1968) 90.
[8] R.J. Madon, J.P. D'Connell, M. Boudart, AIChE J. 24 (1978) 904.
[9] M. Boudart, D.J. Sajkowski, Faraday Discuss. 92 (1991) 57.
[10] E.E. Gonzo, M. Boudart, J. Catal. 52 (1978) 462.
[11] U.K. Singh, M.A. Vannice, J. Catal. 199 (2001) 73.
[12] L. Sordelli, R. Psaro, G. Vlaic, A. Cepparo, S. Recchia, C. Dossi, A. Fusi, R. Zanoni, J. Catal. 182 (1999) 186.
[13] B. Bachiller-Baea, A. Guerrero-Ruiz, P. Wang, I. Rodriguez-Ramos, J. Catal. 204 (2001) 450.
[14] S. Recchia, C. Dossi, N. Poli, A. Fusi, L. Sordelli, R. Psaro, J. Catal. 184 (1999) 1.
[15] P. Reyes, H. Rojas, G. Pecchi, J.L.G. Fierro, J. Mol. Catal. A Chem. 179 (2002) 293.
[16] T. Salmi, P. Maki-Arvela, E. Toukoniitty, A.K. Neyestanaki, K. Tiainen, L. Lindfors, R. Sjoholm, E. Laine, Appl. Catal. A Gen. 196 (2000) 93.
[17] S. Mukherjee, M.A. Vannice, J. Catal. 243 (2006) 108, this issue.
[18] U.K. Singh, M.A. Vannice, J. Catal. 191 (2000) 165.
[19] M. Boudart, G.D. Mariadassou, Kinetics of Heterogeneous Catalytic Reactions, Princeton Univ. Press, Princeton, NJ, 1984.
[20] M.A. Vannice, Kinetics of Catalytic Reactions, Kluwer–Springer, New York, 2005.
[21] U.K. Singh, M.A. Vannice, J. Mol. Catal. A Chem. 163 (2000) 233.
[22] S. Mukherjee, Ph.D. thesis, The Pennsylvania State University, 2005.
[23] M. Boudart, AIChE J. 18 (1972) 465.
[24] J.M. Prausnitz, R.N. Lichtenthaler, E.G. Azevedo, Molecular Thermodynamics of Fluid-Phase Equilibria, second ed., Prentice–Hall, Englewood Cliffs, NJ, 1986.
[25] J.H. Hildebrand, R.L. Scott, The Solubility of Nonelectrolytes, third ed., in: Am. Chem. Soc. Monograph Series, vol. 17, Reinhold, New York, 1950.
[26] S.I. Sandler, Chemical and Engineering Thermodynamics, Wiley, New York, 1989.
[27] H.S. Lo, M.E. Paulaitis, AIChE J. 27 (1981) 842.
[28] U.K. Singh, M.N. Sysak, M.A. Vannice, J. Catal. 191 (2000) 181.
[29] B. Sen, P. Chou, M.A. Vannice, J. Catal. 101 (1986) 517.
[30] R.P. Danner, T.E. Daubert, Manual for Predicting Chemical Process Design Data, AIChE, New York, 1983.